



## Effect of surface preparation and R-group size on the stabilization of lithium metal anodes with silanes

Susanna Neuhold<sup>a,\*</sup>, David J. Schroeder<sup>b</sup>, John T. Vaughey<sup>a</sup>

<sup>a</sup> Chemical Sciences and Engineering Division Argonne National Laboratory, Argonne, IL 60439, United States

<sup>b</sup> Department of Engineering Technology Northern Illinois University, DeKalb, IL 60115, United States

### ARTICLE INFO

#### Article history:

Received 19 December 2011

Received in revised form 18 January 2012

Accepted 21 January 2012

Available online 28 January 2012

#### Keywords:

Anode  
Battery  
Lithium  
Silane  
Cleaning  
Coating

### ABSTRACT

As new applications for lithium-ion batteries emerge into the marketplace, a new emphasis is being placed on developing higher capacity electrodes. Two of the higher capacity technologies under development are lithium–sulfur and lithium–air batteries, both of which, in most configurations, use a lithium metal anode. Building on our previous work extending the cycle life of lithium metal anodes via surface functionalization with silane groups, we have identified two separate regimes for the cycle life enhancements based on size of the silane R-groups. Very small R-groups (TMS) and R-groups bulkier than triphenyl show enhanced cycle life compared to control samples while R-groups between these in size show reduced cycle life. Additionally, we present a comparison between different cleaning methods to optimize the hydroxyl functionalized layer on the lithium metal and the influence of these methods on the stability of lithium metal in EC:EMC electrolyte. A solvent based cleaning approach is shown to substantially improve stability when combined with chlorotrimethyl silane treatment.

Published by Elsevier B.V.

### 1. Introduction

As new uses for lithium-ion batteries come to the forefront, limitations related to theoretical energy capacity of the individual electrodes have become more important [1,2]. This need to identify and develop new high capacity materials has seen dramatic new interest in the lithium silicides, lithium stannides, and conversion materials as well as a renewed interest in metal–air systems [3–10]. Included in this is a new interest in lithium metal anodes [11–15]. Initially studied in the early 1960s, it was eventually replaced as the anode of choice for secondary battery applications by graphitic carbon because of poor electrodeposition properties and extensive reactivity in the cell environment. However, several advantages still make it an attractive anode for battery applications including its high energy density, high capacity, and the lack of processing needed to construct the electrode compared to ones requiring lamination. This utility, as well as advances in characterization over the past decade have opened up new possibilities for stabilizing lithium metal in the presence of the liquid electrolytes [16–18]. Previous efforts focused on producing a coating layer by methods that included in situ polymerization of an electrolyte soluble monomer, in situ formation of Zintl salts, and direct deposition of thin polymer layers onto the surface [19–21]. For many of these

studies, cells showed gradual impedance growth on cycling that was attributable to variables such as SEI film thickening, polymer dissolution, and an unstable surface morphology. In 2007, Marchioni, et al., showed that silane-coated lithium metal exposed to lithium-ion battery organic electrolytes showed enhanced stability compared to untreated samples as judged by electrochemical impedance spectroscopy [15]. The layer was generated by the self-terminating reaction between a chloride substituent on the substituted silane and a proton from the hydroxy-terminated layer on a clean lithium surface. Fig. 1 shows a schematic representation of the reaction mechanism between chlorosilanes and an OH terminated lithium metal surface. This mechanism was confirmed by identification of energy shifts corresponding to Si–O and Li–Cl bonds in XPS and FTIR. Recently this work was extended by Thompson et al. to include cycling data in electrochemical cells against  $\text{Li}_4\text{Ti}_5\text{O}_{12}$  [11]. Consistent with the improved impedance stability, cycle life was found to improve with the silane coated surfaces. The improvements, a two- to three-time enhancement in cycle life, were attributed to reducing the ability of free solvent to reach the active electrode surface. Consistent with such a model, the cycling capacity eventually faded with a slope similar to the untreated samples. The act of continued lithium stripping and re-deposition on the electrode surface gradually disrupted the coatings cohesiveness until the electrode surface resembled untreated lithium metal. To examine this degradation model, the effects of substituent size on cycle life beyond triisopropylsilyl (TIPS) chloride have been examined. While the earlier study determined that

\* Corresponding author. Tel.: +1 6302527138; fax: +1 6302524176.

E-mail address: [neuhold@anl.gov](mailto:neuhold@anl.gov) (S. Neuhold).

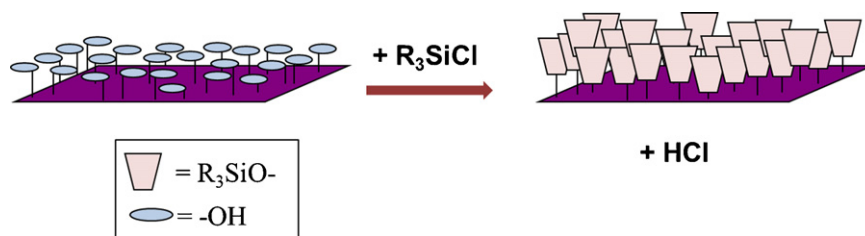


Fig. 1. Schematic representation of the silane coating mechanism.

triisopropylsilyl chloride was less effective than trimethylsilyl chloride presumably due to the larger R-group reducing the number of silicon–oxygen attachments and reducing surface coverage, it is possible that these effects can be overcome by even larger R-groups that are more effective at sterically hindering the approach of electrolyte molecules while being less dependent on the number of surface attachments.

Because the attachment of the silane molecules to the surface is self-terminating and should only be of monolayer thickness the condition of the lithium surface before treatment will strongly influence the quality and performance of the passivation coating. Earlier reports used mechanical action, either scraping with a razor blade [11,15] or with a polyethylene block [22] to remove surface contaminants from the as received lithium metal foil. While this method has been somewhat successful, the ultimate goal of using the silane compounds is to form a continuous passivation film on the lithium surface that is stable and free from defects that allow electrolyte attack. The mechanical cleaning methods have been demonstrated to remove reaction products from the surface but they also embed some of the debris into the bulk of the sample and create other surface inhomogeneities in addition to scraping damage. This may in-turn allow reactions with the electrolyte to proceed more rapidly than it would otherwise. To reduce these surface defects and improve the coatings a chemical cleaning method may be more desirable.

In this study we compare cycling performance and impedance stability of passivation coatings on lithium cleaned both mechanically and chemically. We then evaluate the cycling stability of chemically cleaned lithium metal coated with chlorosilanes with various additional substituents, identifying a trend in cycling stability with substituent size.

## 2. Experimental

Lithium metal foil (FMC-Lithuim, 200  $\mu\text{m}$ ) was received and stored in an argon atmosphere glovebox. Before use the foil was either cleaned abrasively using a razor blade or was cleaned using pentane [11]. For the pentane-based cleaning the lithium electrode was put in 3 mL of the solvent and vigorously stirred for 3 min. After that the electrode was quickly dried in the glove box atmosphere.

For cycling experiments, all samples were cleaned in pentane. After cleaning the surface the metal foil was submerged for 10 s in the appropriate chlorosilane: trimethylsilyl chloride (TMS, Aldrich, 99%), methylsilyl trichloride (Gelest), methylpropylsilyl dichloride (Aldrich, >97%), triethylsilyl chloride (Gelest), methylphenylsilyl chloride (Aldrich, 97%), triisopropylsilyl chloride (Aldrich, 97%), *tert*-butylsilyl chloride (Gelest), triphenylsilyl chloride (Gelest). The triphenylated compound is solid, so a solution in EMC/pentane 1:1 (v/v) was used for the coating process. After coating samples were taken out and allowed to dry in the glovebox.

For the calculation of the molecular volumes of the various substituted silanes, the program molinspiration ([www.molinspiration.com](http://www.molinspiration.com)) was used.

Impedance and cycling data are shown based on the average value of the results from at least three coin cells.

Electrochemical cells (Hohsen, 2032) were made using the silane coated lithium metal as the anode (1.6  $\text{cm}^2$ ),  $\text{Li}_4\text{Ti}_5\text{O}_{12}$  as the cathode and a 1.2 M  $\text{LiPF}_6$  in 3:7 (w/w) EC/EMC electrolyte in a manner recently described [12]. For cycle stability, the cells were cycled at 1.5  $\text{mA cm}^{-2}$  in a voltage window of 1–2 V vs Li. Some cells were also evaluated using AC impedance spectroscopy to determine changes in resistance at the various interfaces during the ageing of the cell. In these experiments, cells were evaluated in the range [ $5 \times 10^{-2}$ – $10^4$  Hz] 1 h after being made and then at ageing times up to one week using an IM6e electrochemical impedance analyzer. The morphology of the lithium samples was investigated using scanning electron microscopy (Jeol JSM-6400).

## 3. Results and discussion

Lithium metal is a reactive element that interacts strongly with many components of its electrochemical cell environment. Within a battery, the lithium metal is known to react instantaneously with the electrolyte components producing a variety of salts, reduced hydrocarbons, and gases [12,16,17]. However, before submersion in the electrolyte, several other species have typically already passivated the lithium metal surface, including  $\text{Li}_3\text{N}$ ,  $\text{Li}_2\text{CO}_3$ , LiOH, and  $\text{Li}_2\text{O}$ . In addition to these salts various spectroscopic measurements have indicated a tightly bound monolayer consisting of hydroxy or carboxylic acid groups on the surface [15]. With the exception of these tightly bound groups, the other surface contaminants are sitting on the surface rather than being bound to it [11,15]. Therefore as the build-up of these contaminants will affect the quality and performance of any coating layer, various methods were investigated to remove them. The simplest method was by stirring in a liquid that is unreactive with lithium metal. Alkali metals are frequently shipped submerged in alkanes because they do not react with them, or do so only very slowly. If a reaction does occur to form Li-alkyls they are known to be soluble in hydrocarbons [23]. After investigating various solvents, *n*-pentane was chosen to clean the lithium surface over other alkanes because its vapor pressure is low enough that it does not evaporate significantly while the lithium is being cleaned but allows the lithium surface to dry quickly when removed from the liquid.

Fig. 2a–d shows lithium foil surfaces after the use of different cleaning methods. All of the pieces of lithium foil tested in this section were dipped in trimethylsilyl chloride prior to removal from the glovebox to reduce the rate of reaction with the atmosphere while being loaded into the SEM. Fig. 2a shows a representative surface of the as-received Li foil. Substantial debris can be seen on the surface. Fig. 2b shows the lithium foil after being repeatedly scraped with a razor blade. Surface damage can be observed with defects on a similar scale to that observed in the as-received lithium. Fig. 2c shows the surface of lithium foil after sitting in pentane for 45 min. The amount of debris is substantially reduced compared to the as-received case to the point that the grain boundaries of the foil can

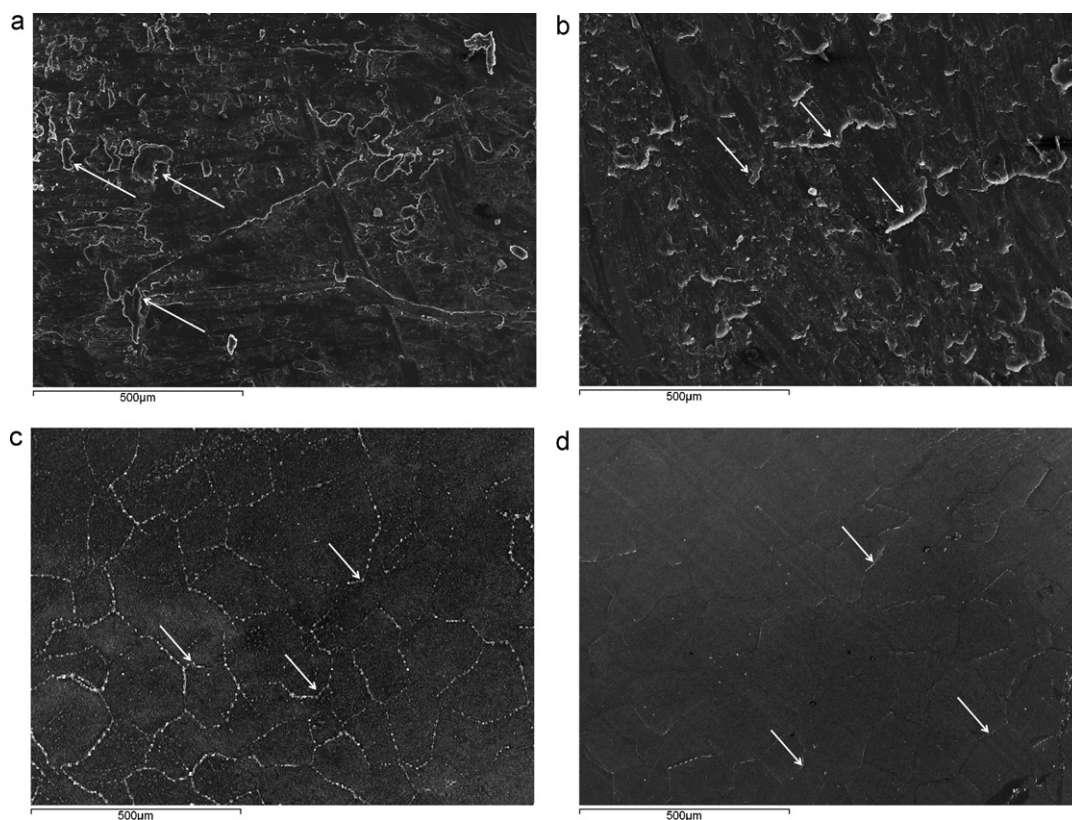


**Fig. 2.** (a) Lithium foil surface as-received (arrows indicate some of the debris on the surface). (b) Lithium foil surface after scraping with a razor (arrows indicate surface defects along the scraping direction). (c) Lithium foil after sitting in pentane for 45 min (arrows indicate grain boundaries). (d) Lithium foil surface after 3 min in stirring pentane (arrows indicate grain boundaries, rolling direction can be seen).

be observed. However, some debris remain at the grain boundaries. Fig. 2d shows the surface of the lithium foil after stirring in pentane for 3 min. Grain boundaries can still be observed but the debris that was observable in the unstirred case has been removed and the surface is now clean enough that marks can be seen on the surface from the foil rolling process.

The next set of images, Fig. 3a–c, shows the surface of lithium foil after exposure to electrolyte following the different cleaning methods. The foils were dipped in trimethylsilyl chloride prior to exposure to the electrolyte. The electrolyte composition was 1.2 M LiPF<sub>6</sub> in 3:7 (w/w) EC/EMC and the exposure time was 45 min. Without any prior cleaning, Fig. 3a, bubbles and reaction products can be clearly seen. They are less easily observable in the case of the razor blade scraped surface, Fig. 3b, but what appears to be the beginning of bubble formation and also cracks in the reacted layer are present. In the pentane cleaned case, Fig. 3c, no bubbles or reaction products are observed but the grain boundaries of the underlying lithium film can no longer be seen indicating that a reaction layer is present. Attempts to collect higher resolution images were not successful because in the case of the uncleaned and razor cleaned surfaces heating from the electron beam caused rapid decomposition and deformation of the surface. In the case of the pentane cleaned surface no features were observable at higher magnification, but the layer did not decompose under the heat of the beam possibly indicating that the reacted layer is substantially thinner or more conductive in this case.

To identify the influence of the TMS coating on the stability of the cells the impedance spectra were recorded for the untreated and treated anodes. In Fig. 4 the values for the resistances  $R_1$  (bulk) and  $R_2$  (interfacial) of a standard Randles cell as shown in Fig. 5 are compared. The resistance values of the uncleaned, razor cleaned, and pentane cleaned lithium foil without TMS treatment were

measured and used as a basis for comparison. These resistances represent the 100% line in Fig. 4. The bars represent the same cleaning conditions relative to their respective baseline values after treatment with TMS. All measurements were made 1 h after the cells were assembled. For the uncleaned lithium foil the treatment with TMS increases the values for the resistances. This is due to the fact that by forming a coating on top of the passivation layer another unbound and inhomogeneous layer is created. For the razor cleaned lithium the resistance values decrease slightly due to passivation of the active sites by TMS. The resistance values for the pentane cleaned and TMS treated cell show a large decrease due to the coating with the chlorosilane. The improvement over the razor cleaned cells is likely the result of a more uniform coating due to the less defective surface, which is shown in Fig. 2b and d. The active surface of the lithium foil can be stabilized by the coating reaction which prevents electrolyte attack.

To further test the effect of the cleaning process on the stability of the reaction layer with electrolyte, electrochemical cells were tested as a function of ageing. An example for a set of typical spectra is shown in Fig. 5 for a coin cell during the ageing period of 168 h after assembling. The values for  $R_1$  are stable, but the values for  $R_2$  increase significantly over this one week time period. Fig. 6 compares  $R_2$  values of cells with and without TMS treatment. Again the values for the untreated cells are used as the 100% line. The  $R_2$  values for the uncleaned lithium foil show an enormous increase after the treatment with TMS, but they seem to stabilize during the ageing process after about one day. While the razor cleaned cells initially show a decrease compared to the untreated cells the advantage is small and after two days the  $R_2$  values become higher than that of the untreated controls. The pentane cleaned cells treated with TMS show significantly decreased starting values for  $R_2$  and this trend is maintained for the duration of the one week test. Again the



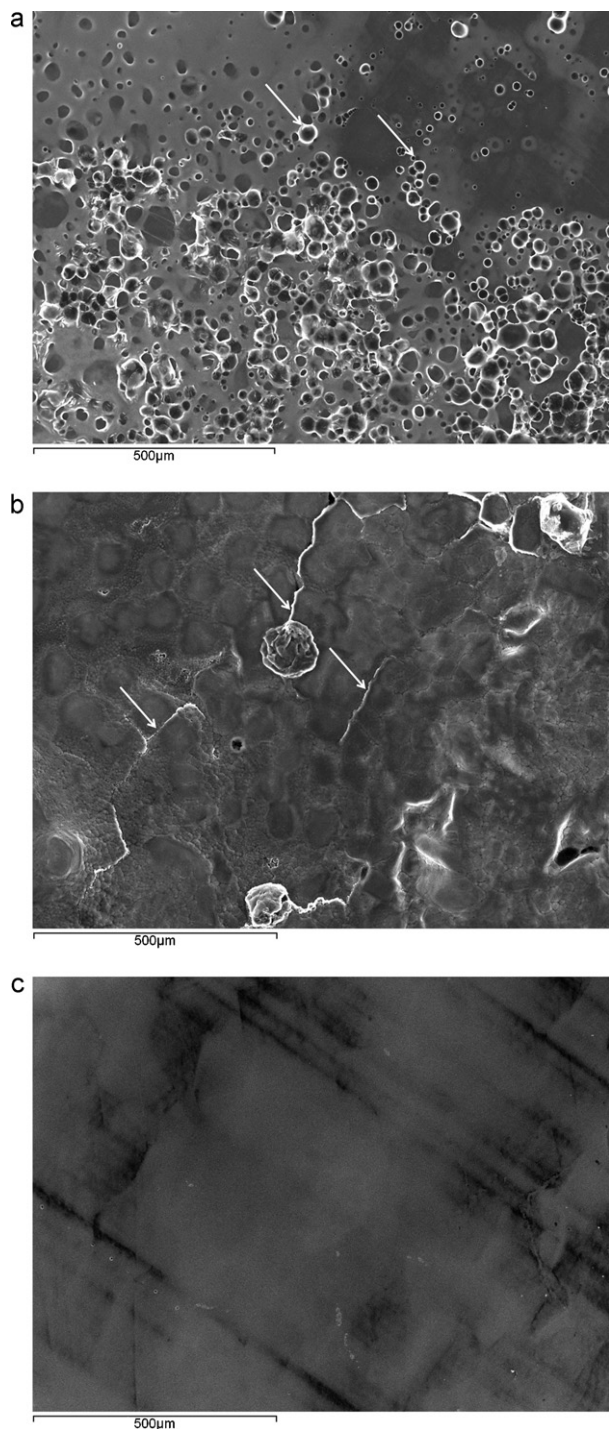


**Fig. 3.** (a) Lithium foil surface (uncleaned) after exposure to Gen 2 electrolyte for 45 min (arrows indicate bubbles in the SEI layer). (b) Lithium foil surface after cleaning with a razor blade and exposing to electrolyte for 45 min. (arrows indicate beam induced cracks in the SEI layer). (c) Lithium foil surface after cleaning in stirred pentane for 3 min and exposing to electrolyte for 45 min (no beam induced cracks or bubbles in the SEI layer can be seen).

improvement over the razor cleaned samples is most likely due to the reduction in defects on the surface that translates to defects in the passivation coating.

Previous work [11,15] identified a stable coating for lithium metal based on the simple surface-driven reaction between the proton of the natural hydroxide terminated layer on clean lithium surface and a variety of substituted chlorosilanes. Because the pentane cleaning process should not be capable of removing tightly

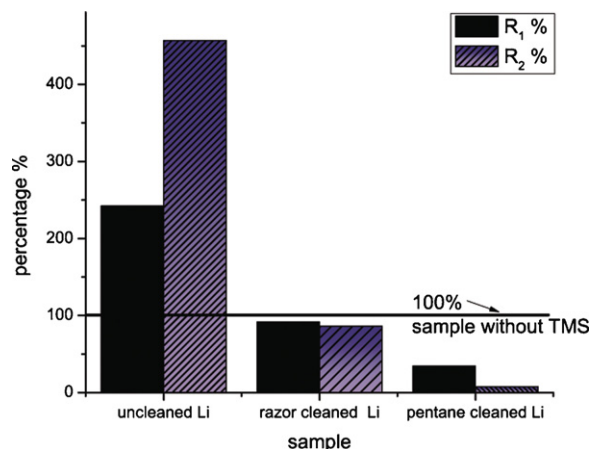


**Fig. 4.** Percentage change of resistances  $R_1$  and  $R_2$  1 h after assembly for the untreated, the scraped, and the pentane cleaned lithium when treated with TMS compared to samples without TMS treatment (100% values).

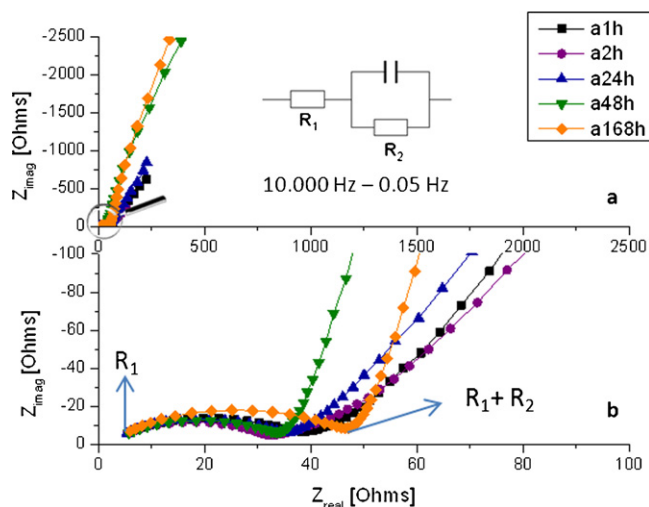


**Fig. 5.** Example of impedance spectra during the ageing of the cell using untreated lithium. Part (a) total range for the spectra and the scheme of a Randles cell. Part (b) zoom into part a explaining the means of the resistances  $R_1$  and  $R_2$ .

bound OH groups on the surface of the lithium metal the mechanism of passivation by the chlorosilanes should be the same as the previously reported one. To verify this, XPS spectra (not shown) were collected for a trimethylsilyl chloride treated sample which

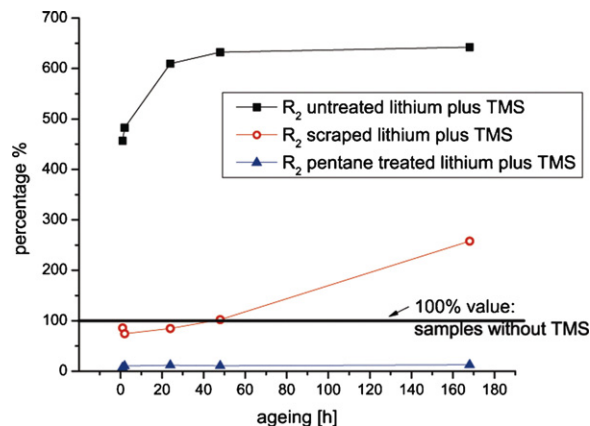


**Fig. 6.** Change of  $R_2$  of the samples with TMS coating in percentage compared to each sample without TMS treatment (100%).

**Table 1**  
Cycling data for different chloro silanes.

Compound	Volume [ $\text{\AA}^3$ ]	Number of cycles to reach 80% capacity	Number of cycles to reach 60% capacity
Me <sub>3</sub> Si-	98.7	166.3	208.7
MeSiCl <sub>2</sub> -	92.6	35.5	86.5
MePropSiCl-	129.0	20.7	41.0
MePhSiCl-	150.5	21.0	54.5
Et <sub>3</sub> Si-	149.1	32.5	57.5
i-Prop <sub>3</sub> Si-	198.8	15.3	27.7
Ph <sub>3</sub> Si-	263.2	49.7	90.3
t-Bu <sub>3</sub> Si-	249.2	88.0	131

had been cleaned with pentane. Peaks consistent with Si–O and Li–Cl formation of approximately one monolayer were observed as expected so no change in reaction mechanism of the chlorosilanes with the surface is occurring regardless of the preparation method. The layer was found to stabilize the surface of lithium in organic electrolytes as identified by a large and sustained drop in the AC impedance in a simple cell for the coated cell vs an uncoated surface. These results were confirmed and extended to show enhancements in cycle life when either trimethylsilyl or triisopropylsilyl chloride were used to treat the lithium metal surface [11]. In that study the TMS coating was shown to increase cycle life more than that of the TIPS chloride due to higher coating density with the TMS chloride. In this study R-group size has been systematically varied to more thoroughly map out the relationship between substituent size and cycle life. All cells prepared for this portion of the study were prepared using pentane cleaned lithium. To ensure that approximately the same amount of lithium was utilized per cycle the mass of Li<sub>4</sub>Ti<sub>5</sub>O<sub>12</sub> cathodes was chosen to be within a few percent of each other.

Coatings were applied by submersing the cleaned lithium anode in the neat (as received) liquid (except for the triphenylated compound). Table 1 shows the R-groups tested and their calculated size. For di- and tri-chlorinated compounds sizes were calculated assuming that only one chlorine reacts with the Li surface. While it is possible that a second chlorine reacts with the surface, this does not significantly influence the volume calculation result. Fig. 7 shows the number of cycles required to reduce the cell capacity to 80% and 60% of their original value vs calculated R-group size. Zero represents the pentane cleaned, untreated, control. Points represent the average value of three cells. On the small R-group side of the graph, TMS chloride shows a substantial increase in cycle life in comparison to the untreated control. It also gives much better cycle life (average of 217 cycles) than what our group achieved previously with TMS chloride where 80% retention of initial capacity was reached at approximately 120 cycles. The difference between

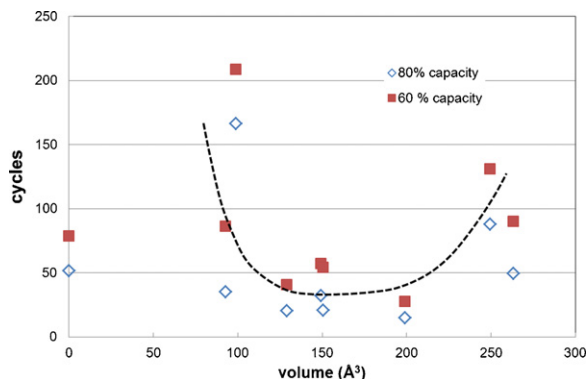


**Fig. 7.** Relative size of R-group vs the number of cycles required for capacity to 80% and 60% of its initial value.

those cells and the ones measured here is only the pentane cleaned surface preparation.

The different behavior of the Me<sub>3</sub>SiCl (98.7  $\text{\AA}^3$ ) and Me<sub>2</sub>SiCl<sub>2</sub> (92.6  $\text{\AA}^3$ ) shows, that not only the R group size is important, but also the number of functional groups being able to react with the surface. The dichloro compound shows decreased cycling stability which could have two causes. If the second chloride functionality reacts with the surface it decreases the density of the monolayer and therefore steric hindrance to electrolyte molecules and if it does not it remains available for side reactions.

As R-group size is increased above that of TMS, coating cycle life drops off but increases again at substantially higher R-group size. A drop in cycle stability with increasing molecular volume is expected because the coating density should decrease. However, between 125 and 200  $\text{\AA}^3$  the cycle life is depressed even below that of the control. While this is not understood it could be the result of the coating interfering with the development of the natural passivation film. As R-group size increases further, above 200  $\text{\AA}^3$ , the cycle stability improves. Even though the density of the coating on the surface probably continues to decrease the increased ability of large substituents to interfere with the approach of the electrolyte sterically outweighs the effect of lower coating density.

#### 4. Conclusions

We have demonstrated the use of a new cleaning method for preparing lithium metal anodes for treatment and cycle life testing using pentane. These pentane cleaned surfaces show enhanced stability in the electrolyte during ageing when treated with TMS chloride compared to the abrasive cleaning method. The new cleaning process was used to evaluate the effect of the R-group size of various silyl chloride compounds on cycle life. Very small R-groups (TMS) and R-groups bulkier than triphenyl show enhanced cycle life compared to the pentane cleaned control while R-groups between these in size show reduced cycle life.

#### Acknowledgements

This work was supported by the ILIRP Program, Batteries for Transportation Technologies (BATT) Program, Office of Vehicle Technologies, Office of Energy Efficiency and Renewable Energy of the U.S. Department of Energy. SEM images were recorded using the equipment at the Electron Microscopy Center for Materials Research, Argonne National Laboratory; a US Department of Energy Office of Science Laboratory operated under Contract no. DE-AC02-06CH11357 by UChicago Argonne, LLC.

#### References

- [1] Stewart, S.G. Srinivasan, V. J. Newman, J. Electrochem. Soc. 155 (2008) A664.
- [2] P.H.L. Notten, F. Roozenboom, R.A.H. Niessen, L. Baggefto, Adv. Mater. 19 (2007) 4564.
- [3] M.N. Obrovac, L.J. Krause, J. Electrochem. Soc. 154 (2007) A103.
- [4] B. Key, M. Morcrette, J.M. Tarascon, C.P. Grey, J. Am. Chem. Soc. 133 (2011) 503.
- [5] I.T. Lucas, E. Pollack, R. Kostecki, Electrochem. Commun. 11 (2009) 2157.
- [6] A.N. Jansen, J. Clevenger, A. Baebler, J.T. Vaughey, J. Alloys Compd. 509 (2011) 4457.
- [7] L.Y. Beaulieu, S.D. Beattie, T.D. Hatchard, J.R. Dahn, J. Electrochem. Soc. 150 (2003) A419.
- [8] N. Yamakawa, M. Jiang, B. Key, C.P. Grey, J. Am. Chem. Soc. 131 (2009) 10525.
- [9] J. Chen, F.Y. Cheng, Acc. Chem. Res. 42 (2009) 713.
- [10] J.T. Vaughey, A.M. Geyer, N. Fackler, C.S. Johnson, K. Edstrom, H. Bryngelsson, R. Benedek, M.M. Thackeray, J. Power Sources 174 (2007) 1052.
- [11] R.S. Thompson, D.J. Schroeder, C.M. López, S. Neuhold, J.T. Vaughey, Electrochem. Commun. 13 (2011) 1369.
- [12] C.M. López, J.T. Vaughey, D.W. Dees, J. Electrochem. Soc. 156 (2009) A726.
- [13] E. Zinigrad, E. Levi, H. Teller, G. Salitra, D. Aurbach, P. Dan, J. Electrochem. Soc. 151 (2004) A111.
- [14] Y. Shimada, K. Okita, Y. Okuno, Y. Iriyama, Electrochemistry 78 (2011) 427.
- [15] F. Marchionni, K. Star, E. Menke, T. Buffeteau, L. Servant, B. Dunn, F. Wudl, Langmuir 23 (2007) 11597.

- [16] M. Ishikawa, K. Inoue, N. Yoshimoto, M. Morita, *Electrochemistry* 71 (2003) 1046.
- [17] M.Z. Xue, J. Yao, S.C. Cheng, Z.W. Fu, *J. Electrochem. Soc.* 153 (2006) A270.
- [18] R.N. Mason, M. Smith, T. Andrews, D. Teeters, *Solid State Ionics* 118 (1999) 129.
- [19] L. Yang, C. Smith, C. Patrissi, C.R. Schumaker, B. Lucht, *J. Power Sources* 185 (2008) 1359.
- [20] M. Maxfield, T.R. Jow, S. Gould, M.G. Sewchok, L. Shacklette, *J. Electrochem. Soc.* 135 (1988) 299.
- [21] M. Ishikawa, M. Morita, Y. Matsuda, *J. Power Sources* 68 (1997) 501.
- [22] G.A. Umeda, E. Menke, M. Richard, K.L. Stamm, F. Wudl, B. Dunn, *J. Mater. Chem.* 21 (2011) 1593.
- [23] D. Braun, W. Betz, W. Kern, *Makromol. Chem.* 42 (1) (1960) 89–95.